APPLICATION OF A NEW ALGORITHM FOR PREDICTION AND MODELLING OF MULTIPHASE BEHAVIOR: A CASE STUDY OF SOME PROTOTYPE NATURAL GAS SYSTEMS

Roumiana P. STATEVA and Stefan G. TSVETKOV

Institute of Chemical Engineering,
Bulgarian Academy of Sciences, 1113 Sofia, Bulgaria

Received March 15, 1993
Accepted September 28, 1993

The prediction and modelling are studied of complex multiphase behavior of four prototype ternary mixtures typically encountered in cryogenic processing of natural gases, with a new approach for solving the isothermal multiphase flash problem. The method includes a rigorous method for thermodynamic stability analysis as the first step and an efficient phase identification procedure as the second. The new algorithm provides an accurate global description of phase behavior of the studied LNG systems, and excellent agreement of the results obtained with experimental data.

In processing natural gas systems (i.e. the systems rich in methane and ethane), the presence of a second liquid phase in a customarily liquid–vapor mixtures can often cause problems and upset the expected design performance. Though only a limited number of immiscible binary systems (methane–n-hexane, methane–n-heptane, to name the most prominent ones) are relevant to natural gas processing, liquid–liquid–vapor (LLV) behavior can and does occur under certain conditions in ternary and higher realistic liquefied natural gas (LNG) systems even when none of the constituent binaries themselves exhibit such a behavior. It is also known that the addition of nitrogen to miscible LNG systems can induce immiscibility and this necessarily affects the process design for these systems.

The recent active interest in the use of nitrogen gas to pressurize oil reservoirs to enhance recovery has resulted in natural gas process streams rich in nitrogen, which are likely to display the LLV behavior. Investigators have studied experimentally ternary prototype LNG systems containing nitrogen, and a lot of excellent data have been published[1 – 3]. However, in order to help further understanding the possible occurrence of multiphase equilibria in LNG process systems, it is necessary to acquire the knowledge of their phase behavior and of the variety of critical end point boundaries through an ability to predict, model and calculate them. This is a challenging and rewarding task.

The present study deals with the prediction and modelling of the multiphase behavior of four prototype ternary mixtures typically encountered in cryogenic processing of

natural gases: methane–ethane–nitrogen, methane–propane–nitrogen, methane–n-butane–nitrogen and methane–n-pentane–nitrogen (the species in the systems being ordered as solvent–solute–second solvent). Firstly, the question of the topography of the multiphase equilibrium behavior of the systems in thermodynamic phase space and the nature of the phase boundaries will be addressed. Then, the computational procedure will be outlined. Finally, results of the phase equilibrium predictions and calculations will be presented.

THEORETICAL

Topography of Multiphase Behavior

The type of the LLV region displayed by the systems depends on whether they contain an immiscible binary or not[4].

The two systems nitrogen–methane–n-butane and nitrogen–methane–n-pentane do not exhibit immiscibility in any of their binary pairs and are topologically similar, sharing the same sort of boundaries. A schematic diagram of the P–T projection of the LLV space is shown in Fig. 1. The three-phase region is "triangular" (a surface in the thermodynamic phase space with two degrees of freedom) and is bounded from above by a K-point locus (L–L=V), from below by a LCST locus (L=L–V) and at low temperatures by a Q-point locus (S–L–L–V). These three loci intersect at invariant points for the ternary system: the K-point and LCST loci – at a tricritical point t (L=L=V), while the Q-point locus terminates at point A (S–L–L=V) from above and point B (S–L=L–V) from below, respectively.

The systems nitrogen–methane–ethane and nitrogen–methane–propane, however, contain binary pairs which exhibit LLV behavior (they are LLV immiscible in them-

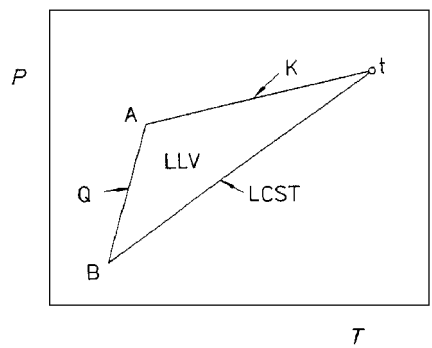

FIG. 1
Schematic diagram of *P–T* projection of LLV space for CH_4–n-C_4H_{10}–N_2 and CH_4–n-C_5H_{12}–N_2 mixtures (no constituent binary LLV behavior present)

selves). In such cases, the triangular LLV region (Fig. 1) is changed because a truncation of the phase space is introduced (see ref.[4]). The immiscible pairs C_2H_6–N_2 and C_3H_8–N_2 differ in end points from the classical case and they span the LLV space from a position on the LCST locus to a position on the Q-point locus[4]. Methane is of intermediate volatility when compared to the components of the constituent immiscible binaries and creates a three-phase LLV surface, extending from the binary LLV locus upward in temperature. The topographical nature of the regions of immiscibility for the systems methane–ethane–nitrogen and methane–pentane–nitrogen is shown in Fig. 2.

Application of the Algorithm

Modelling of the complex phase behavior of LNG systems requires a suitable thermodynamic model and a robust and efficient computational algorithm. In the present work, the application of a recently proposed[5,6,7] method for performing phase stability and multiphase flash calculations is illustrated.

The computer algorithm is based on a new approach to solving the isothermal multiphase flash problem when the number, identity and composition of the phases present at equilibrium are unknown in advance. Thus, two interlinked subproblems have to be solved: firstly, the phase configuration of the system with the minimum Gibbs energy has to be identified; secondly, the compositions of the equilibrium phases at the specified temperature and pressure have to be calculated.

To efficiently realize these tasks, the new method applies two sequential calculational procedures:

1. The first procedure is a rigorous method for thermodynamic stability analysis, performed *only once* and on the initial system only (see ref.[5]). Should instability be detected, the second procedure is applied:

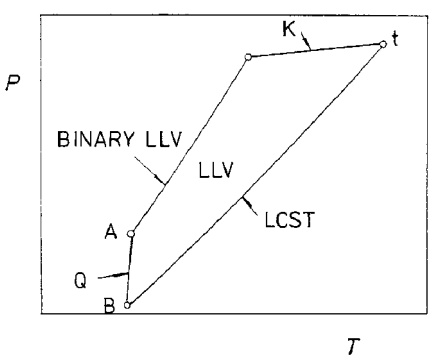

FIG. 2
Schematic diagram of *P–T* projection of LLV space for CH_4–C_2H_6–N_2 and CH_4–C_3H_8–N_2 mixtures

2a. It uses a sequence of two-phase liquid–liquid and/or liquid–vapor flashes until the phase configuration with the minimum Gibbs energy is determined.

2b. In case LLV is identified as the stable equilibrium, an additional LLV flash is run to obtain the correct phase distribution.

The procedures implement an equation of state (EOS) as the thermodynamic model of both the liquid and vapor equilibrium phases.

The stability check is based on the well-known tangent-plane criterion (see refs[8,9]), but applies a different objective function. The key point is to locate all (the maximum possible number of the) zeros ($\boldsymbol{y}^*$) of a functional $\Phi(\boldsymbol{y})$ formed

$$\Phi(\boldsymbol{y}) = \sum_{i=1}^{N_c} [k_{i+1}(\boldsymbol{y}) - k_i(\boldsymbol{y})]^2 \quad , \tag{1}$$

where

$$k_i(\boldsymbol{y}) = \ln \varphi_i(\boldsymbol{y}) + \ln y_i - h_i \quad i = 1,2,...,N_c \quad , \tag{1a}$$

$$h_i = \ln z_i + \ln \varphi_i(\boldsymbol{z}) \quad i = 1,2,...N_c \quad , \tag{1b}$$

and we assume $k_{N_c+1}(\boldsymbol{y}) = k_1(\boldsymbol{y})$.

From Eq. (*1*) follows directly, that

min $\Phi(\boldsymbol{y}) = 0$,

when $k_1(\boldsymbol{y}^*) = k_2(\boldsymbol{y}^*) = ... = k_{N_c}(\boldsymbol{y}^*)$.

The rigorous stability analysis which acts as a useful precursor is exercised once and on the initial system only. It provides the information which is analyzed and used to gain an insight into the nature of the system possible phase equilibria. The latter is further applied to arrange efficiently successive two-phase flash calculations, and obtain a trustworthy and easy solution of the phase identification task and a set of excellent initial estimates for the LLVE computations.

If multiple zeros of the functional with liquid and a vapor phase identification are obtained, this means that the initial system is either LL, LV or LLV. To determine correctly the phase identification and component distribution, the following algorithm is suggested:

1. Run a liquid–liquid (LL) and a liquid–vapor (LV) flash calculations.

2. Calculate the molar Gibbs energy which corresponds to the LV solution according to

$$G_{\text{Feed}} = G_V \alpha + G_L (1 - \alpha) \tag{3}$$

and for the LL solution according to

$$G_{\text{Feed}} = G_{L_1} \alpha + G_{L_2} (1 - \alpha) \ . \tag{3a}$$

3. If

$$G_{\text{Feed}}^{\text{LL}} < G_{\text{Feed}}^{\text{LV}} \qquad (4)$$

continue with Step *4*, otherwise proceed to Step *7*.

4. Perform a new liquid–vapor flash calculation – (LV)′. Flash the L_2 phase. (Here and further on, the liquid phase, rich in the most volatile component, will be referred to as L_2 phase).

If the (LV)′ flash computation converges at this stage with a phase split (β) outside the physically acceptable bounds $0 \leq \beta \leq 1$, this indicates that the initial system is a stable liquid–liquid. Furthermore, its correct phase compositions and amounts are determined. STOP.

If the (LV)′ flash computation converges with a phase split (β) inside the physically acceptable bounds $0 \leq \beta \leq 1$, the initial LL system is identified as liquid–liquid–vapor. Continue with Step *5*.

5. Perform a liquid–liquid flash calculation $(L_1L_2)''$ on the liquid phase of the (LV)′ solution of Step *4*.

6. Run a liquid–liquid–vapor flash. Use as initial estimates the following composition vectors $\boldsymbol{x}_{L_1''}$, $\boldsymbol{x}_{L_2''}$, $\boldsymbol{y}_{V'}$. STOP.

7. Perform a liquid–liquid (LL)′ flash computation. Split the liquid phase from the LV solution of Step *1*.

If the (LL)′ flash computation converges at this stage with a phase split (β) outside the physically acceptable bounds $0 \leq \beta \leq 1$, the initial system is classified as a stable liquid–vapor and its correct phase compositions and amounts are also determined. STOP. Otherwise, the system is identified as an LLV. Continue with Step *8*.

8. Perform a liquid–vapor flash calculation (LV)˜. Flash the vapor phase of the LV solution of Step *1* to obtain a vapor phase and a liquid phase (L)˜ rich in the most volatile component.

9. Perform a liquid–liquid flash (LL)″ on the L˜ phase of Step *8*.

10. Run liquid–liquid–vapor flash computations. Use as initial estimates the following composition vectors $\boldsymbol{x}_{L_1''}$, $\boldsymbol{x}_{L_2''}$, $\boldsymbol{y}_{V\tilde{}}$. STOP.

Paradigm (see Chart A) summarizes schematically all cases encountered and the steps performed by the above proposed algorithm when solving the isothermal multiphase flash problem.

The steps of the algorithm mimic the process of phase splitting and new phase formation in a heterogeneous multicomponent mixture until a state with the lowest possible Gibbs energy is obtained. Moreover, physical reasons to accept or discard from further consideration a certain mathematical solution (as a non-physical, “pseudo” one) are implemented in the algorithm, which is an additional asset.

A set of excellent initial estimates for the two-phase liquid–liquid–vapor and liquid–liquid flash calculations are obtained as a result of the stability analysis (stage *1*). Fur-

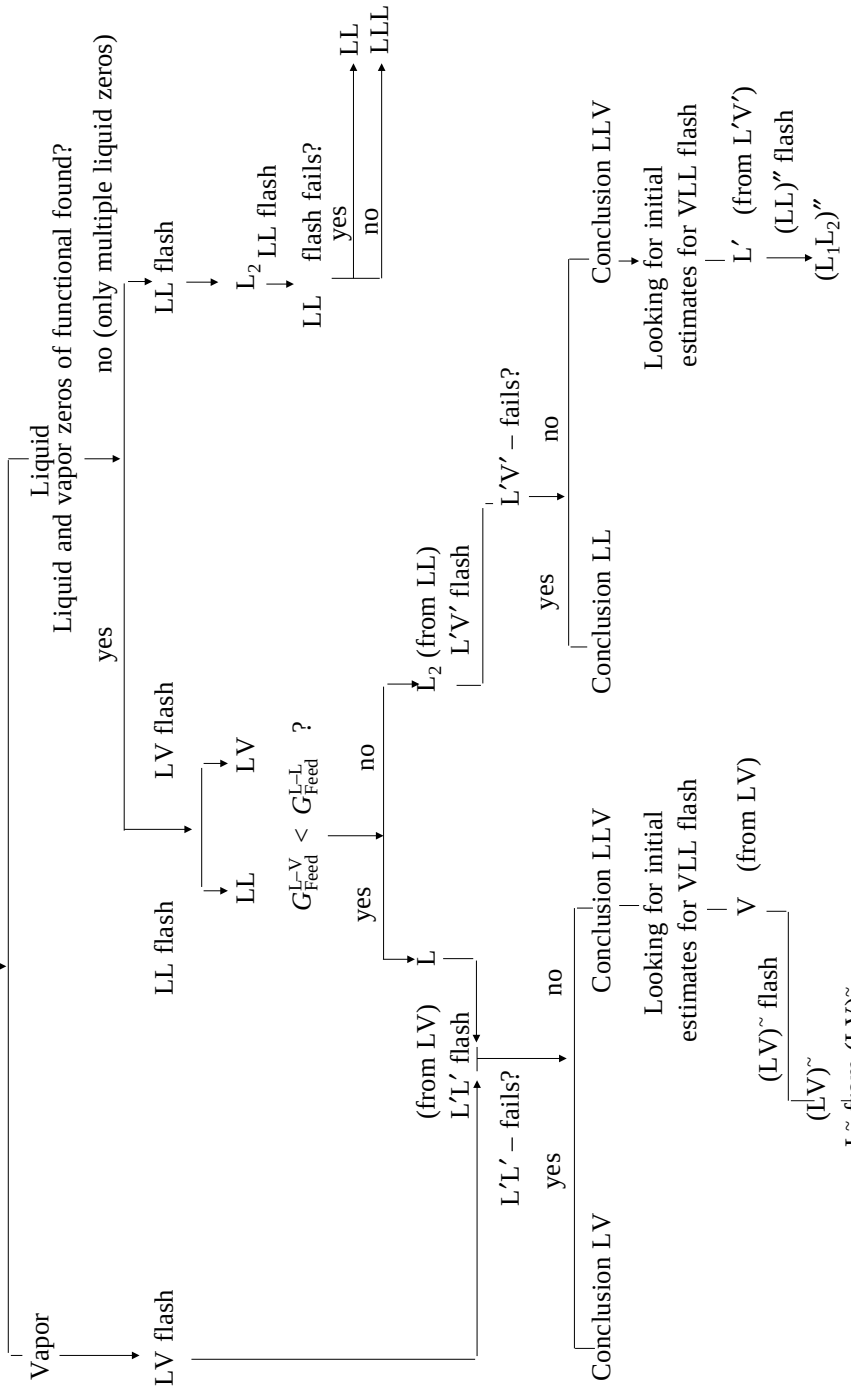
Feed is unstable
Vapor
LV flash
Liquid
Liquid and vapor zeros of functional found?
yes
no (only multiple liquid zeros)
LL flash
LV flash
LL flash
LV
LL
L_2 LL flash
$G^{L-V}_{Feed} < G^{L-L}_{Feed}$?
LL flash fails?
yes
no
LL
LLL
yes
no
L
(from LV)
L′L′ flash
L_2 (from LL)
L′V′ flash
L′V′ – fails?
yes
no
L′L′ – fails?
yes
no
Conclusion LV
Conclusion LLV
Looking for initial estimates for VLL flash
V (from LV)
(LV)˜ flash
(LV)˜
L˜ from (LV)˜
(LL)″ flash
(L_1L_2)″
Conclusion LL
Conclusion LLV
Looking for initial estimates for VLL flash
L′ (from L′V′)
(LL)″ flash
(L_1L_2)″

CHART A

thermore, the set of initial estimates for the LLV flash, obtained after stage *2a*, are so close to the true solution that (as it will be demonstrated in a later section) the calculations converge very quickly and steadily.

The Soave–Redlich Kwong cubic equation of state (SRK CEOS) is used as the thermodynamic model of the four investigated prototype ternary mixtures. The binary interaction parameters k_{ij} used are those obtained from the literature[10], with the exception of the k_{ij} coefficient for the nitrogen–n-butane binary. The interaction parameter in that case was calculated according to the correlation proposed by Moysan et al.[11] since the value recommended in Knapp et al.[10] led to erroneous results.

The obtained results are surprisingly good taking into consideration that the same set of k_{ij} (obtained by processing LV data only) have been used to predict and model LV, LL and LLV equilibria.

RESULTS AND DISCUSSION

The new algorithm is utilized to predict and model the phase and volumetric behavior of the four ternary prototype LNG systems. Liquid- and vapor-phase compositions and molar volumes are reported as a function of temperature and pressure within the three-phase region and along the boundaries over a wide temperature range.

Table I presents the set of initial estimates for the LLV flash routine and the calculated three-phase compositions for the methane–ethane–nitrogen mixture at T = 125 K and P = 2.53 MPa.

Table II presents the set of initial estimates and the calculated three-phase compositions for the methane–propane–nitrogen mixture at T = 123 K and P = 2.33 MPa.

Tables III and IV give the equilibrium compositions and molar volumes of the methane–n-butane–nitrogen and methane–n-pentane–nitrogen mixtures, simulated by the algorithm.

The effect of pressure (studied values ranging from 2.9 MPa $\leq P \leq$ 3.5 MPa) on the LLV equilibrium of methane–ethane–nitrogen mixture at T = 129 K is shown on the isothermal pressure–composition prism (Fig. 3, simulated by the computer). This prism has been constructed by stacking triangular phase diagrams generated at different pressures. Each diagram shows only the three phase LLV region at a specified pressure (the two-phase regions, corresponding to L_1V, L_2V and L_1L_2 equilibria, and bounding the three-phase triangle are not depicted in order not to overcrowd the figure).

At a pressure lower than 2.9 MPa, the system exhibits two-phase vapor–liquid equilibrium only (the lowest phase diagram at P = 2.9 MPa); at P = 2.939 MPa a three-phase liquid–liquid–vapor region appears which persists up to P = 3.521 MPa.

The combined effect of temperature and pressure on the LLV equilibrium of methane–propane–nitrogen mixture at three different temperatures T_1 = 138 K, T_2 = 140 K, T_3 = 142 K, and pressure values ranging from 2.960 MPa to 4.243 MPa, is shown on a set of three pressure–composition prisms (Fig. 4, simulated by the computer). At T = 138 K,

the LLVE appears at P = 2.960 MPa and persists up to P = 3.750 MPa; at T = 140 K, LLVE appears at P = 3.158 MPa and extends to P = 4.145 MPa, and at T = 142 K, LLVE exists for pressure values ranging from 3.355 MPa to 4.243 MPa.

Excellent experimental data for all the systems studied are available in the literature[1–3]. The experimental phase compositions (mole fraction of nitrogen) for the methane–propane–nitrogen, methane–n-butane–nitrogen and methane–n-pentane–nitrogen mixtures at T = 134 K, T = 138.97 K, T = 150 K, respectively, and various pressures, are com-

TABLE I
Phase calculations for CH_4–C_2H_6–N_2 mixture at T = 125 K, P = 2.53 MPa

Component	Feed	Component mole fractions							
		Initial split		Initial estimates			Converged results		
		Liquid	Vapor	L_1	L_2	V	L_1	L_2	V
CH_4	0.15	0.2302	0.0487	0.2232	0.1693	0.0486	0.2214	0.1671	0.046
C_2H_6	0.15	0.2681	$8.1 \cdot 10^{-5}$	0.3804	0.0773	$7.6 \cdot 10^{-4}$	0.3845	0.0760	$8.3 \cdot 10^{-4}$
N_2	0.7	0.5017	0.9504	0.3964	0.7534	0.9506	0.3941	0.7569	0.9528

Since multiple zeros of functional are found, LL and LV flash calculations are run (follow Paradigm in Chart A). Gibbs energy calculations: $G_{\text{Feed}}^{\text{L–V}} < G_{\text{Feed}}^{\text{L–L}}$. Phase split: $\alpha_{\text{LV}} = 0.4418$; $\beta_{(\text{LL})'} = 0.2648$. Phase split three phase flash: $\gamma_{\text{I}} = 0.4118$; $\gamma_{\text{II}} = 0.3081$.

TABLE II
Phase calculations for CH_4–C_3H_8–N_2 mixture at T = 123 K, P = 2.33 MPa

Component	Feed	Component mole fractions							
		Initial split		Initial estimates			Converged results		
		L_1	L_2	L_1	L_2	V	L_1	L_2	V
CH_4	0.2	0.2384	0.1627	0.2557	0.1784	0.0559	0.2557	0.1784	0.0559
C_3H_8	0.3	0.6032	0.0057	0.5830	0.0064	$1.43 \cdot 10^{-5}$	0.5830	0.0064	$1.42 \cdot 10^{-5}$
N_2	0.5	0.1584	0.8316	0.1613	0.8152	0.9441	0.1613	0.8152	0.9441

Since multiple zeros of functional are found, LL and LV flash calculations are run (follow Paradigm in Chart A). Gibbs energy calculations: $G_{\text{Feed}}^{\text{L–L}} < G_{\text{Feed}}^{\text{L–V}}$. Phase split: $\alpha_{\text{LL}} = 0.5074$; $\beta_{(\text{LV})'} = 0.1278$. Phase split three phase flash: $\gamma_{\text{I}} = 0.3432$; $\gamma_{\text{II}} = 0.5108$.

pared with the predicted values in Figs 5 – 7. The calculated curves are obtained by repeated flash calculations, and the converged solution, in each case, is obtained in less than 5 iterations. As it can be seen, the calculated and the measured compositions are in very good agreement.

Our studies confirm that the extent of the domain of three-phase behavior of the system methane–ethane–nitrogen is considerably less than that of the system methane–propane–nitrogen. This latter system has a three-phase region extent comparable to that of the methane–n-butane–nitrogen system, though the topography of their LLV beha-

TABLE III
Phase calculations for CH_4–n-C_4H_{10}–N_2 mixture

Phase	x_{CH_4}	$x_{C_4H_{10}}$	x_{N_2}	v, $cm^3\ mol^{-1}$
		I = 120 K; P = 1.40 MPa		
L_1	0.5393	0.3286	0.1321	52.97
L_2	0.5149	0.0145	0.4706	42.48
V	0.1111	$4.5 . 10^{-8}$	0.8889	551.30
		I = 159.52 K; P = 5.04 MPa		
L_1	0.5677	0.2832	0.1491	55.35
L_2	0.5071	0.0038	0.4891	73.27
V	0.4253	0.0006	0.5741	107.87

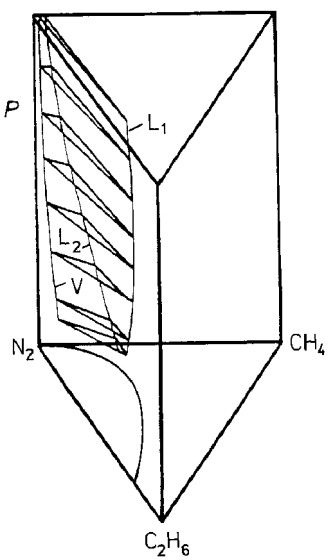

FIG. 3
Effect of pressure on three-phase equilibrium for CH_4–C_2H_6–N_2 at T = 129 K

vior differs as pointed out in a previous paragraph. In turn, extent in temperature–pressure space diminishes somewhat as n-butane is replaced by the heavier species n-pentane. It seems apparent therefore that propane and n-butane are prime contributors to the LLV immiscibility in the nitrogen-rich LNG mixtures.

TABLE IV
Phase calculations for CH_4–n-C_5H_{12}–N_2 mixture

Phase	x_{CH_4}	$x_{C_5H_{12}}$	x_{N_2}	v, cm^3 mol^{-1}
		I = 140 K; P = 1.86 MPa		
L_1	0.6829	0.2104	0.1067	53.98
L_2	0.7617	0.0467	0.1916	46.07
V	0.3421	$7.9 \cdot 10^{-8}$	0.6579	468.2
		I = 180 K; P = 5.05 MPa		
L_1	0.7443	0.1841	0.0716	58.30
L_2	0.8059	0.0054	0.1887	76.70
V	0.7496	0.0006	0.2498	120.13

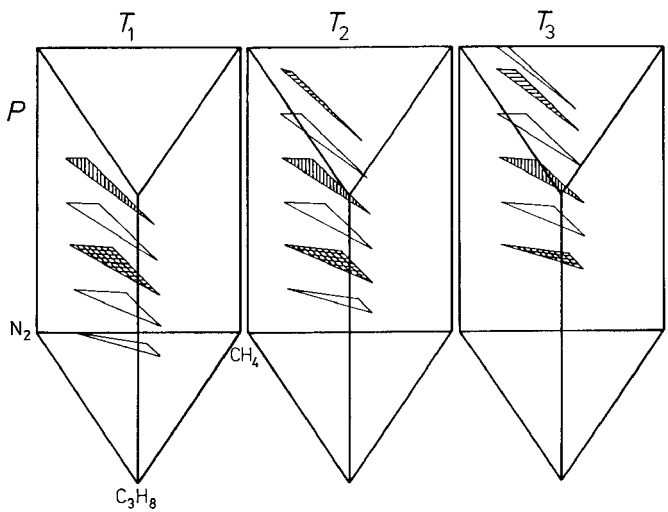

FIG. 4
Pressure–composition prisms for CH_4–C_3H_8–N_2 at T_1 = 138 K, T_2 = 140 K and T_3 = 142 K. Identical hatching of three phase triangles notify identical values of pressure in different prisms

The pressure–temperature (PT) projection of the methane–propane–nitrogen mixture is presented in Fig. 8. The system contains an immiscible binary pair propane–nitrogen and hence the liquid–liquid–vapor equilibrium curve for the propane–nitrogen binary, the critical endpoint L=L–V curve and the K-point locus are shown (see also Fig. 2).

The LLV behavior over the entire range of temperatures and pressures studied for the methane–n-butane–nitrogen system is represented in Fig. 9. Since the system does not contain an immiscible binary pair (compare with Fig. 1), the PT projection includes the predicted three-phase triangular region bounded by a critical endpoint L–L=V curve (K-points locus), a Q-point locus, and a critical solution temperature curve (CST).

CONCLUSIONS

The new method and algorithm provide an accurate global description of the phase behavior of the four studied prototype ternary LNG systems. It is important to note that not only the regions of the multiphase behavior that have been observed in the experiment have been correctly predicted but that there is a good quantitative agreement between calculated and measured phase compositions. This work has also shown that higher-order critical phenomenon (e.g. tricritical points in ternary mixtures) can be described by a CEOS, for example SRK CEOS.

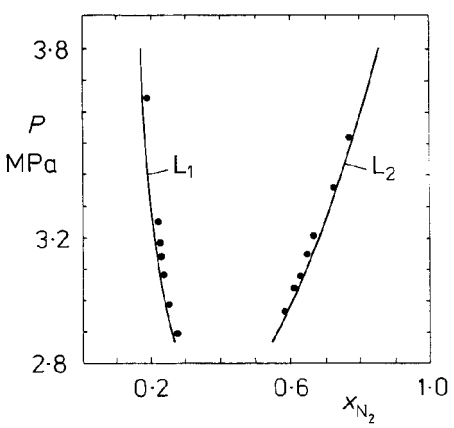

FIG. 5
Comparison of L_1 and L_2 compositional data for CH_4–C_3H_8–N_2 at T = 134 K; — calculated in this study, ● experimental results[1]

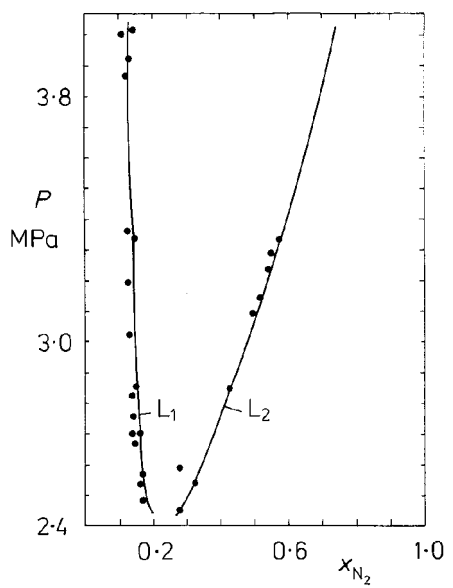

FIG. 6
Comparison of L_1 and L_2 compositional data for CH_4–n-C_4H_{10}–N_2 at T = 138.97 K; — calculated in this study, ● experimental results[2]

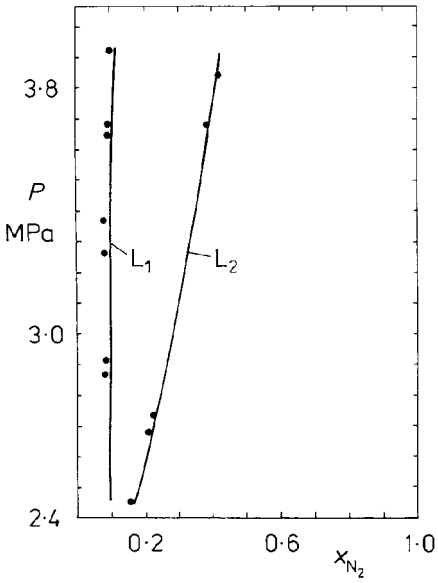

FIG. 7
Comparison of L_1 and L_2 compositional data for CH_4–n-C_5H_{12}–N_2 at T = 150 K; — calculated in this study, ● experimental results[3]

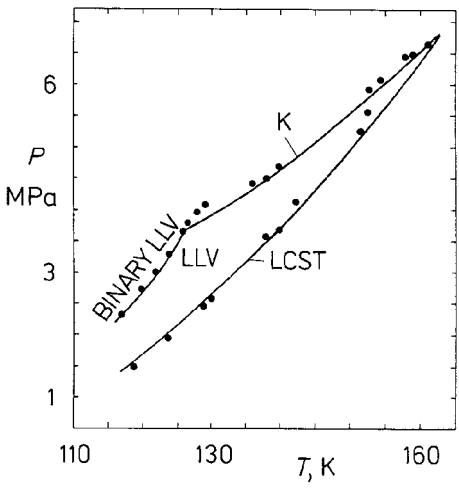

FIG. 8
P–T diagram for CH_4–C_3H_8–N_2; — calculated in this study, ● experimental results[1]

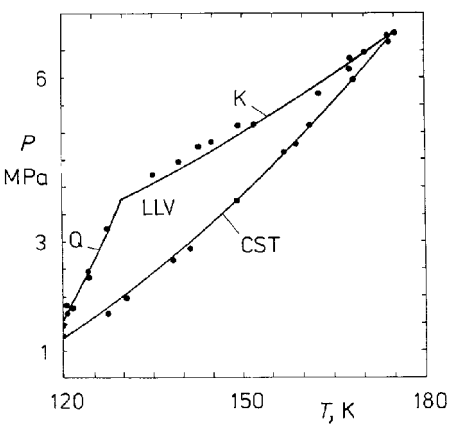

FIG. 9
P–T diagram for CH_4–n-C_4H_{10}–N_2. Above 150 K, CST locus is composed of LCST points. Below 150 K, CST boundary changes character to UCST locus. — Calculated in this study; ● experimental results[2]

The proposed new method and algorithm easily reproduce the complete spectrum of the fluid phase equilibria demonstrated by the studied systems. Moreover, they have proved to be trustworthy, effective and efficient, and can be used successfully to simulate and design different processes involving LNG systems.

SYMBOLS

CST	critical solution temperature
G	molar Gibbs energy
$k_1(\boldsymbol{y})$	function of chemical potential difference, Eq. (*1a*)
k^*	number corresponding to $\boldsymbol{y}^*$
k_{ij}	binary interaction parameter, SRK CEOS
K	K-point or upper critical end point of L_1L_2V region occurring when L_2 phase becomes critically identical with vapor phase (L–L=V)
L_1	liquid phase rich in solute
L_2	liquid phase lean in solute
LLV	liquid–liquid–vapor used to indicate L_1L_2V equilibrium and region
LCST	lower critical solution temperature occurring when the L_1 and L_2 phases become critically identical
N_c	total number of components in mixture
P	pressure
Q	quadruple point, occurs whenever there is equilibrium coexistence of four-phases, herein as S, L_1, L_2,V phases
S–L–L–V	solid–liquid–liquid–vapor equilibrium
t	tricritical point, the intersection of LCST and K-point locus, whereby the three phases L_1, L_2, V are in critical identity (there is $L_1 = L_2 = V$ criticality)
T	temperature
S	solid phase
UCST	upper critical solution temperature
v	molar volume
V	vapor phase
$\boldsymbol{y}$	mole fraction vector, Eq. (*1*)
$\boldsymbol{y}^*$	zero of functional $\Phi(\boldsymbol{y})$ for initial system
$\boldsymbol{x}$	mole fraction vector, equilibrium compositions
$\boldsymbol{z}$	mole fraction vector, initial system
α, β	phase split (two phase flash)
γ	phase split (three phase flash)
$\Phi(\boldsymbol{y})$	functional, Eq. (*1*)
φ	fugacity coefficient, component i

Superscripts

L–L	liquid–liquid equilibrium
L–V	liquid–vapor equilibrium
L–L–V	liquid–liquid–vapor equilibrium
*	corresponding to zero of functional $\Phi(\boldsymbol{y})$
(′), (″)	indicates sequence of LL flashes run by Identification procedure (follow Paradigm, Chart A)

(′), (˜) indicates sequence of LV flashes run by Identification procedure (follow Paradigm, Chart A)

Subscripts

Feed referring to system under consideration
L liquid
V vapor

REFERENCES

1. Llave F. M., Luks K. D., Kohn J. P.: J. Chem. Eng. Data *32*, 14 (1987).
2. Merrill R. C., Luks K. D., Kohn J. P.: Adv. Cryog. Eng. *29*, 49 (1984).
3. Merrill R. C., Luks K. D., Kohn J. P.: J. Chem. Eng. Data *29*, 272 (1984).
4. Luks K. D., Merrill R. C., Kohn J. P.: Fluid Phase Equilib. *14*, 193 (1983).
5. Stateva R. P., Tsvetkov St. G.: Technol. Today *4*, 233 (1991).
6. Stateva R. P., Tsvetkov St. G.: Collect. Czech. Chem. Commun. *57*, 1362 (1992).
7. Stateva R. P., Tsvetkov St. G.: Can. J. Chem. Eng., submitted.
8. Baker L. E., Pierce A. C., Luks K. D.: Soc. Pet. Eng. *22*, 731 (1982).
9. Michelsen M. L.: Fluid Phase Equilib. *9*, 1 (1982).
10. Behrens D., Eckermann R. (Eds): *Chemistry Data Series*, Vol. VI, p. 771. DECHEMA, Frankfurt 1982.
11. Moysan J. M., Paradowski H., Vidal J.: Chem. Eng. Sci. *41*, 2069 (1986).

Translation revised by J. Linek.